Available online at www.sciencedirect.com
ScienceDirect
Geochimica et Cosmochimica Acta 71 (2007) 2436–2447
Geochimica et Cosmochimica Acta
www.elsevier.com/locate/gca

Mass spectrometric and quantum chemical determination of proton water clustering equilibria

Alexander Likholyot, Kono H. Lemke, Jamey K. Hovey, Terry M. Seward *

Institute of Mineralogy and Petrology, ETH Zürich, Universitätsstrasse 16, CH-8092 Zurich, Switzerland

Received 1 November 2006; accepted in revised form 16 February 2007; available online 14 March 2007

Abstract

We report on the thermochemistry of proton hydration by water in the gas phase both experimentally using high-pressure mass spectrometry (HPMS) and theoretically using multilevel G3, G3B3, CBS-Q, CBS-QB3, CBS/QCI-APNO as well as density functional theory (DFT) calculations. Gas phase hydration enthalpies and entropies for protonated water cluster equilibria with up to 7 waters (i.e., $n \leqslant 7 H_3O^+ \cdot (H_2O)_n$) were observed and exhibited non-monotonic behavior for successive hydration steps as well as enthalpy and entropy anomalies at higher cluster rank numbers. In particular, there is a significant jump in the stepwise enthalpies and entropies of cluster formation for n varying from 6 to 8. This behavior can be successfully interpreted using cluster geometries obtained from quantum chemical calculations by considering the number of additional hydrogen bonds formed at each hydration step and simultaneous weakening of ion–solvent interaction with increasing cluster size. The measured total hydration energy for the attachment of the first six water molecules around the hydronium ion was found to account for more than 60% of total bulk hydration free energy.
© 2007 Elsevier Ltd. All rights reserved.

1. INTRODUCTION

Interactions between ions and solvent molecules play a key role in the stepwise solvation of the hydronium ion by water

$$H^+(H_2O)_n + H_2O = H^+(H_2O)_{n+1} \quad (1)$$

and are anticipated to provide fundamental insight into the nature of proton transfer processes (Marx, 2006) and properties of the single molecule to bulk (liquid phase) solvation (Gilligan and Castleman, 2003). Reaction (1) has also received considerable attention for its significance in the formation of so-called Eigen- ($H_9O_4^+$) and Zundel-type ($H_{13}O_6^+$) (Eigen, 1963; Zundel and Metzer, 1968) ion clusters (Fig. 1), its role in proton mobility (Eigen and De Maeyer, 1958), diffusion of protons during formation of solvent defect structures in water (Marx et al., 1999) and formation of protonated water bridges in biological membranes (Meot-Ner et al., 1998) and its importance in ion chemistry in the ionosphere (Asmis et al., 2003; Aplin and McPheat, 2005). Protonated water clusters have been identified in planetary atmospheres and interstellar media (Klemperer and Vaida, 2006). In addition, neutral water clusters, for example, the water dimer (Curtiss et al., 1979) are also considered to play an important role in the photochemistry and radiation balance of the atmosphere and hence, on climate (Vaida et al., 2001; Pfeilsticker et al., 2003). Absorption of solar radiation by water vapour (e.g., clusters) comprises the most important overall contribution to the greenhouse effect (Sennikov et al., 2005). Protonated water clusters occur in the D region (60–90 km) of the stratosphere–ionosphere (Ferguson and Fehsenfeld, 1969; Ferguson and Arnold, 1981) and have been implicated in the formation and kinetics of hydrated radical complexes involved in ozone destruction. The role of ionic clusters in atmospheric chemistry and climate change is currently receiving considerable attention.

Proton hydration also plays an important role in hydrogen-bonding phenomena in high temperature low-density, supercritical water (Matubayasi et al., 1997; Kalinichev

* Corresponding author. Fax: +41 (0)1 632 1334.
E-mail address: tseward@erdw.ethz.ch (T.M. Seward).

0016-7037/$ - see front matter © 2007 Elsevier Ltd. All rights reserved.
doi:10.1016/j.gca.2007.02.022

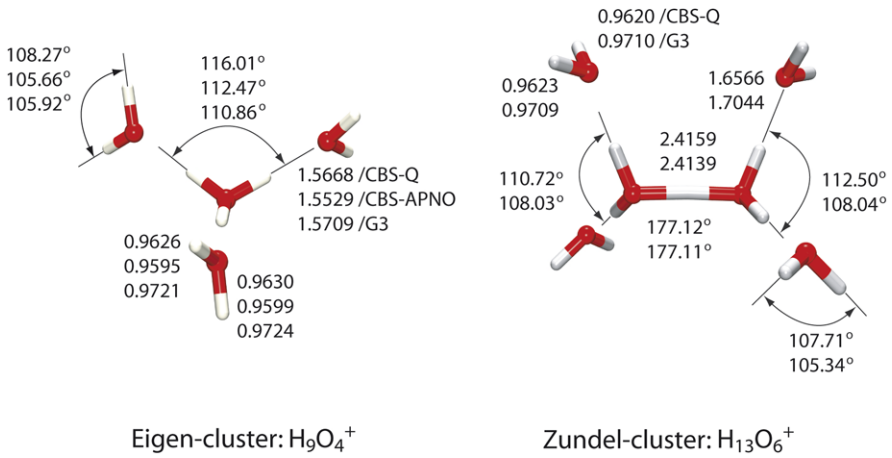

Fig. 1. CBS-Q, CBS/QCI-APNO and G3 gas phase geometries of hydrated Eigen $H_9O_4^+$ and Zundel $H_{13}O_6^+$ ions.

and Churakov, 2001), with fundamental geochemical applications. Protonated water clusters have also been demonstrated to be present in water vapor over boiling water (Carlon, 1979, 1980, 1982) and corresponding clustering equilibria have been applied for the calculation of the pH of steam (Klots, 1984). The pH of steam in low-density supercritical aqueous media is premised upon proton water clustering equilibria. Thus, the study of water clusters by combined *ab initio* methods and experiment provides insight into many molecular-scale geochemical processes, such as proton transfer, solvent competition and ligand switching reactions in ionic clusters (e.g., $NH_4^+ \cdot (H_2O)_m(H_2S)_n$ and $H_3O^+ \cdot (H_2O)_m(H_2S)_n$) and solvation in van der Waals clusters (e.g., $NH_3 \cdot (H_2O)_n$ and $CO_2 \cdot (H_2O)_n$) (Lemke and Seward, 2006). More importantly, these water cluster moieties are important conceptual building blocks upon which we can base our modern thinking of solvation in water over a wider range of temperatures and pressures.

The role of water cluster moieties in other geochemical environments is of fundamental importance but is currently poorly understood and seldom considered. For example, in phase-separating hydrothermal (magmatic) systems at supercritical conditions, ionic and molecular species partition between a more saline (dense) and less dense, volatile-enriched phase. In high temperature porphyry systems, Heinrich et al. (1999) have shown that certain metals such as copper concentrate into the volatile-rich (less dense) phase. It has been observed, that the volatility of CuCl (and other metal complexes) is enormously enhanced in presence of water vapour over wide ranges of temperature (Archibald et al., 2002) as a result of the formation of $CuCl(H_2O)_n$ water clusters. Molecular metal–water clusters are important in the transport of ore metals in low density supercritical fluids and steam as noted by Williams-Jones et al. (2002) and probably account for much of the trace element transport signatures of volcanic gases. The well-known solubility of NaCl in sub- and supercritical water vapour (Bischoff and Rosenbauer, 1986; Armellini and Tester, 1993) is fundamentally determined by the formation of simple NaCl–water clusters containing up to 8 water molecules (Suleimenov and Seward, 2006). Interestingly, protonated water clusters have also been implicated in the formation of ionospheric precursors of earthquakes (Pulinets and Boyarchuk, 2004; Pulinets et al., 2006) and the magic number water clathrate structures hold promise as new hydrogen storage materials (Mao and Mao, 2004).

Kebarle and coworkers carried out the earlier definitive investigations of protonated water clusters (Kebarle et al., 1967; Cunningham et al., 1972; Lau et al., 1982). Their HPMS measurements yielded the first stepwise binding energies for small ($n \leqslant 6$) protonated water clusters, provided insight into the effect of temperature and humidity on equilibrium constants for reaction (1) and demonstrated the existence of distinct solvent-shell filling effects. These types of studies have prompted a suite of experimental efforts, especially noteworthy here are pulsed high-pressure mass spectrometric studies (P-HPMS) (Meot-Ner and Field, 1977; Hiraoka et al., 1986; Meot-Ner and Speller, 1986) and more recently, IR spectroscopic studies (Jiang et al., 2000; Miyazaki et al., 2004; Shin et al., 2004; Lin et al., 2005; Headrick et al., 2005) of protonated water clusters. The reader is referred to Meot-Ner (2005) and Chang et al. (2005) for a thorough review on ionic-hydrogen bonding, hydronium water clusters, cluster structures and corresponding thermochemical properties as well as to Christie and Jordan (2001, 2002), Kuo and Klein (2005), Mella et al. (2005) and Kochanski et al. (1997) for some of the recent quantum chemical studies on protonated water clusters. The review by Chang et al. (2005) also covers selected aspects of quantum chemistry, such as for instance, B3LYP density functional methods that have been employed to calculate equilibrium structures and energies of "magic number" $H^+(H_2O)_{21}$ and $H^+(H_2O)_{28}$ clusters (Wu et al., 2005). However, it should be noted that given the large number of coexisting stable isomers for $n > 6$, it is currently impractical to conduct global minima searches using high accuracy *ab initio* methods for such large size molecules. Recent advances in the application of *ab initio* theory by the Pople (Curtiss et al., 1991) and Petersson (Nyden and Petersson, 1981) groups now permit the calculation of equilibrium structures and energies of small-sized ($n \leqslant 4$) ion–water clusters to an accuracy of ± 2 kJ mol^{-1} (Pickard et al., 2005).

Building on reported studies for protonated water clusters as well as on our recent experimental investigation of

halide hydration (Likholyot et al., 2005b), we have reexamined the clustering equilibria of the hydronium ion with water using our recently constructed HPMS facility (Likholyot et al., 2005a), which incorporates some important design improvements. We have also complimented our experimental studies by performing a series of high accuracy *ab initio* calculations employing the G3 (Curtiss et al., 1998), G3B3 (Baboul et al., 1999), CBS/QCI-APNO (Montgomery et al., 1994), CBS-QB3 (Montgomery et al., 1999) and CBS-Q (Ochterski et al., 1996) model chemistries as well as density functional theory calculations (DFT) at the B3LYP level of theory to obtain equilibrium structures and incremental binding energies for selected isomers of protonated water clusters of rank $n \leqslant 8$.

2. EXPERIMENTAL

The construction of the HPMS apparatus, description of operation, and discussion of errors associated with the HPMS experiments are given in our recent report (Likholyot et al., 2005a). The samples were prepared by injection of distilled water with a calibrated microliter syringe into a 5 L gas mixing glass bulb kept at 140 °C and filled with methane. After an equilibration period of ~20 min, the mixture was allowed to flow from the bulb through the ion source. Ions were produced by a short electron beam pulse. Ions leaving the ion source were mass-selected by the mass spectrometer and their intensities were recorded as a function of time after each electron pulse. Ionizing electron pulse widths of 5–70 μs and electron gun filament currents of 4–5 A were used. The time between electron pulses was maintained in the range 0.5–2 ms. This time was normally chosen to be 20% longer than the overall lifetime of the ions in the ion source as determined by the decrease to zero intensity of measured ionic abundances. Tests were also made using longer time periods that yielded identical ionic abundance ratios. On average, between 100 and 300 thousand pulses were necessary to collect reasonable ionic profiles. For this system, the ion signal in pulsing mode was weak due to rapid diffusion of the produced ions to the source walls. It was concluded that a larger internal ion source volume would be advantageous for proton hydration experiments. The measurements were taken over a temperature range from +540 °C to −22 °C. At the lowest temperature, ion abundances became non-measurable. At 580 °C, considerable spontaneous ionization was observed even when the electron gun and all ionization gauges were turned off. Partial water pressures of 0.04–0.3 mbar were used. The ion source pressure was kept in the range 1.5–6 mbar, where lower pressures were used at lower temperatures. These pressures were chosen to keep the gas number density in the ion source constant throughout the experimental temperature range. At low ion source pressures, the reactants and products may be assumed to behave as perfect gases. For a standard state pressure of 1000 mbar, the equilibrium constant for reaction (1) is given by:

$$K_{n,n+1} = \frac{I_{n+1} \cdot 1000}{I_n \cdot p(\mathrm{H_2O})} \tag{2}$$

where $p(H_2O)$ is the water partial pressure in the ion source, and I_{n+1} and I_n are measured intensities of $H^+(H_2O)_{n+1}$ and $H^+(H_2O)_n$, respectively, after equilibrium has been established. The ratio of measured ionic intensities should remain constant with time when equilibrium conditions apply. In an effort to ensure that equilibrium was indeed established, equilibrium constants were measured as a function of water partial pressure and overall ion source pressure and were found to be independent of these pressures within experimental errors.

Once the equilibrium constants at several temperatures are determined, the enthalpy and entropy changes for the reaction (3) may be calculated in the conventional way using the well-known relation:

$$\ln K = -\frac{\Delta H^\circ}{R}\left(\frac{1}{T}\right) + \frac{\Delta S^\circ}{R} \tag{3}$$

If the van't Hoff plots exhibit linearity, as was the case for the studied clustering reactions, then the enthalpy and entropy changes are obtained from the isochore slopes and *y*-intercepts.

The clustering reactions that were measured in this study span the rank range from for $1 \leqslant n \leqslant 7$; the lowest rank number corresponds to the hydration of the hydronium ion with one water molecule. It should be mentioned that measurement of the first hydration step $n = 0$ (i.e., the hydration of a proton with one water molecule) would require extremely high temperatures, as the enthalpy change for this step obtained from quantum chemical calculations is around 690 kJ mol^{-1}. Consequently, our experimentally measured equilibria were those involving the hydration of hydronium ion ($n = 1$). We refer here to proton hydration because our quantum chemical calculations also include the first hydration step.

3. COMPUTATIONAL METHODS

All *ab initio* calculations were performed using the GAUSSIAN03 (Frisch et al., 2003) program on a cluster at the Competence Center for Computational Chemistry (C4) and on a HP Superdome9000 located in the Department of Computer Science, both at the ETH. All molecular structures were processed using MOLDEN (Schaftenaar and Noordik, 2000). We employed the G3, G3B3, CBS/QCI-APNO, CBS-QB3 and CBS-Q *ab initio* model chemistries as well as the B3LYP density functional theory based method for our ion cluster calculations. The energy of proton hydration ($n = 1$) at 298 K was calculated from the ideal gas enthalpy 2.5RT and the Sackur-Tetrode expression for the entropy.

The G3 method is a 7 step model chemistry that starts with a HF/6-31G(*d*) geometry optimization, followed by a HF/6-31G(*d*) frequency calculation and a second geometry optimization at the MP2(full)/6-311G(*d*) level. The MP2 geometry is then used for four single point calculations (SPC), at the QCISD(T,E4T)/6-31G(*d*), MP4/6-31+G(*d*), MP4/6-31G(*2df,p*), and MP2(full)/GT level. The CBS/QCI-APNO procedure begins with a UHF/6-311G(*d,p*) geometry optimization, a frequency calculation at the HF/6-311G(*d,p*) level and a second geometry optimization

at the higher QCISD/6-311G(*d*,*p*) level. As in the G3 model chemistry, the final geometry (QCISD) in the CBS/QCI-APNO method is then used in four SPCs, at the QCISD(T)/6-311++G(2*df*,*p*), MP2 = Full/CBSB6, HF/CBSB5A, and MP2/CBSB5 level.

The CBS-Q methods represents the more cost effective all three model chemistries, but nevertheless yields high accuracy (i.e., <6.5 kJ mol^{-1} deviation from the G2 testset) thermochemistry and is therefore well-suited for calculations on larger hydronium–water clusters. The seven step CBS-Q routine involves four SPCs on a MP2/6-31G(*d*) geometry and a HF/6-31G(*d*) frequency calculation.

We also applied the high accuracy multilevel model chemistries CBS-QB3 (Montgomery et al., 1998) and G3B3 (Baboul et al., 1999) that use density functional based structures and frequencies. The CBS-QB3 routine involves the use of the B3LYP/CBSB7 method, while the G3B3 method builds on the B3LYP/6-31G(*d*) method. It should be mentioned that both the G-*n* and the CBS-*x* methods do not suffer from any basis set superposition errors, i.e., they are by definition BSSE-free and thus do not require counterpoise-type procedures to correct for basis set truncation (Mayer, 1999). It is also noted that theoretical binding energies of hydrogen bonded clusters without BSSE corrections often more closely reproduce experimental clustering equilibria as BSSE and basis set truncation errors cancel (Dunning, 2000; Masamura, 2001); see Xantheas (2005) for a review on BSSE correction procedures and cluster binding energies. Also, given the relatively minor contribution of vibrational anharmonicity to the binding energies in water clusters as demonstrated by Diri et al. (2005) (i.e., anharmonicity corrections to theoretical binding energies of $(H_2O)_6$ are less than 4 kJ mol^{-1}), we have not incorporated such corrections into our theoretical results. In addition to our model chemistry calculations, we also performed density functional calculations with the B3LYP functional employing Becke's gradient corrected exchange functional, the Lee–Yang–Parr correlation functional and the 6-311G** basis set. Subsequent frequency calculations performed using the same level of theory were used to verify that an optimized structure was a minimum on the potential energy surface and for calculation of thermochemical data at different temperatures. All frequencies in our DFT work were scaled using a common factor of 0.89.

The knowledge of cluster vibrational frequencies and moments of inertia for protonated water clusters allows for calculation of the energy distribution for the clusters and, in particular, calculation of the fraction, f_{ex}, of clusters having energies above the dissociation threshold energy (Likholyot et al., 2005a). This information is important for experimental studies that measure clustering equilibria as it allows the choice of experimental conditions where clusters are most stable and hence will not undergo unimolecular dissociation during mass analysis. The problem of unimolecular dissociation in high-pressure mass spectrometry was considered in detail previously by (Sunner and Kebarle, 1981). Once vibrational frequencies and moments of inertia of a cluster are known, the excited fraction, f_{ex}, can be calculated:

$$f_{ex} = 1 - \frac{1}{Q}\sum_{E_i=0}^{H} P(E_i)\exp\frac{-E_i}{kT} \quad (4)$$

where ΔH for the cluster formation reaction approximates the threshold energy, Q is the partition function, and $P(E_i)$ is the multiplicity of the state with energy E_i. Zero-point energy is the reference energy level. Because of the requirement for angular momentum conservation, the overall rotations were assumed to be unable to provide energy for dissociation. As such, only vibrational frequencies were used in energy calculations and sums of states. Multiplicities of vibrational states were computed using the Beyer-Swinehart algorithm for counting states (Stein and Rabinovitch, 1973). The excited fraction calculations were performed for all protonated water clusters at different temperatures. The optimal choice of experimental temperature ranges used to study each reaction was aided by the results of these calculations. Experimental measurements were performed at sufficiently low temperatures such that the excited fractions did not exceed 1%.

4. RESULTS AND DISCUSSION

4.1. Experimental results

Typical temporal profiles for recorded ion signals are shown in Fig. 2. These profiles have been normalized to the total ion intensity in order to cancel the effect of signal decay due to diffusion of ions to the ion source walls. Establishment of equilibrium was always extremely fast. As can be seen in Fig. 2, equilibrium was established approximately 100 μs after the electron pulse. Experimental results are presented as van't Hoff isochore plots in Fig. 3. Errors in the calculated entropies due to mass discrimination in ion sampling (Likholyot et al., 2005a) were small compared with experimental errors and the corresponding corrections were not included here.

4.2. Quantum chemical results

Optimized hydronium water cluster geometries calculated at the CBS-Q theory level with rank numbers

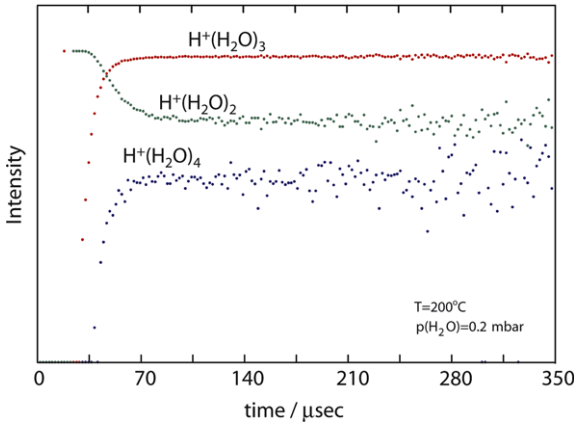

Fig. 2. Ionic profiles normalized to total ion intensity for protonated water clusters after the ionization pulse.

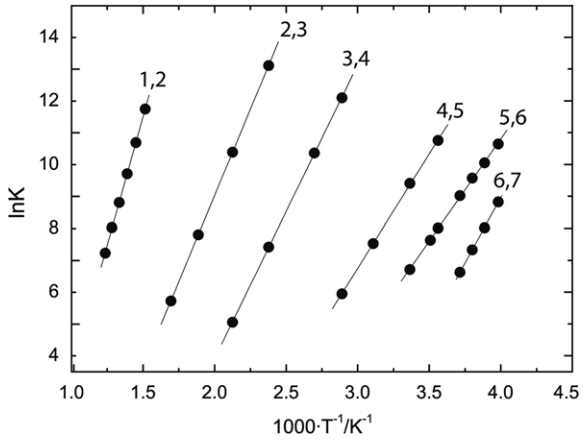

Fig. 3. Experimental van't Hoff plot for protonated water clusters; the notation 1,2 refers to the addition of one water molecules to the hydronium ion (i.e., $n = 1$ refers to H_3O^+; $n = 2$ refers to $H_5O_2^+$).

$1 \leqslant n \leqslant 7$ are shown in Fig. 4 and corresponding thermochemical properties are listed in Table 1. As may be seen from Fig. 1, clusters are formed around a very stable hydronium ion in which a proton forms a covalent bond with the water molecule ($n = 1$). Because of the non-spherical central ion, protonated water clusters lack spherical symmetry, in contrast with water clusters of metal ions. The three hydrogen atoms of hydronium ion form hydrogen bonds with solvent water yielding loosely bound structures. Structures shown in Fig. 4 were found to be the most stable isomers, although there exists an increasing number of alternative stable isomers with increasing cluster size. Incremental hydration enthalpies and entropies calculated from G3, G3B3, CBS/QCI-APNO, CBS-QB3, CBS-Q and DFT results and averaged over corresponding experimental temperature ranges are given in Table 2 along with experimental values. It should be noted that in Table 2, the enthalpies and entropies obtained from theoretical methods are for reactions between two single cluster molecules and a water molecule, whereas experimental enthalpies and entropies are based on populations of isomers of $H^+(H_2O)_n$ and $H^+(H_2O)_{n+1}$ clusters. Fractions of clusters with energies exceeding the dissociation threshold energy were calculated as a function of temperature and are shown in Fig. 5. These results were used in determining the best experimental temperature ranges where no significant fraction of observed clusters would dissociate during mass analysis.

4.3. Discussion

Comparison of our results from theoretical calculations with experimental thermochemical data for the stepwise hydration of the hydronium ion is given in Fig. 6. The overall agreement between the present and earlier experimental data is good, except for the (6,7) hydration step.

There is a good agreement in stepwise trends between the present experimental data and our quantum chemical results. An analysis of the excited fractions within the experimental ranges used in the work of Kebarle et al. (1967) shows that beginning with $n = 5$, their experiments were performed under conditions where excited fractions were larger than 5%. In addition, it is possible that earlier HPMS designs had larger errors in temperature and ion source pressure measurement as discussed in Likholyot et al. (2005a). If clusters of size, $n + 1$, have larger excited fraction than clusters of size, n, the observed stepwise enthalpy change will have a larger magnitude than the true value because excited fractions decrease with decreasing temperature. Analysis of the excited fraction for ions involved in the (6,7) step shows that clusters with $n = 7$ have a smaller excited fraction than clusters with $n = 6$ within the temperature employed by Kebarle et al. (1967). In such a case, unimolecular dissociation for the (6,7) step within the given temperature range would lead only to a slight decrease in the magnitude of the enthalpy change. It appears that the discrepancy between the enthalpy change for the (6,7) step as reported by Kebarle et al. (1967) and our experimental values stems from temperature and ion source pressure uncertainties in their earlier measurements. The measurement of the (7,8) hydration step by Kebarle et al. (1967) was carried out over a temperature range where the excited fraction for $n = 8$ is very large. The dependence of the excited fraction on temperature, however, is weak within this experimental temperature range. The net effect of unimolecular dissociation would be a shift of the van't Hoff plot downward leading to a change only in the entropy. Indeed, the enthalpy change for the (7,8) step from Kebarle et al. (1967) agrees well with our quantum chemical results, however, the magnitude of the entropy change is almost twice that predicted by the calculations.

Measurements carried out by Lau et al. (1982) were done under the conditions where no significant unimolecular dissociation was present. However, the lowest temperature in their experiments was −60 °C where water vapor could begin to condense in the ion source. We observed such condensation at −45 °C in our experimental study of chloride (Likholyot et al., 2005b) as did Hiraoka et al. (1988). The ice vapor pressure is 0.130 mbar at −40 °C, 0.039 mbar at −50 °C and only 0.011 mbar at −60 °C (Lide, 1996). If water condenses in the ion source, then the real partial pressure of water is lower than expected and the calculated equilibrium constants would be smaller. Because this effect would become more pronounced at lower temperatures, the van't Hoff plots would be less steep, leading to smaller magnitudes for the calculated enthalpy change. This might be an explanation for the large discrepancy between results by Lau et al. (1982) and our data for the (6,7) step as well as for smaller discrepancies in the preceding two hydration steps, since the corresponding van't Hoff plots by Lau et al. (1982) also extend into the lower temperature region for these reactions.

While our experimental enthalpies reveal minor systematic deviations from both density functional (B3LYP) and *ab initio* (CBS-*x* and G-*n*) results, they do follow the same stepwise trends. These trends can be interpreted through the number of stabilizing hydrogen bonds formed at each step. The overall decrease in the absolute value of the enthalpy change with increasing size is due to the weakening of proton–water or hydronium–water hydrogen bonds when a

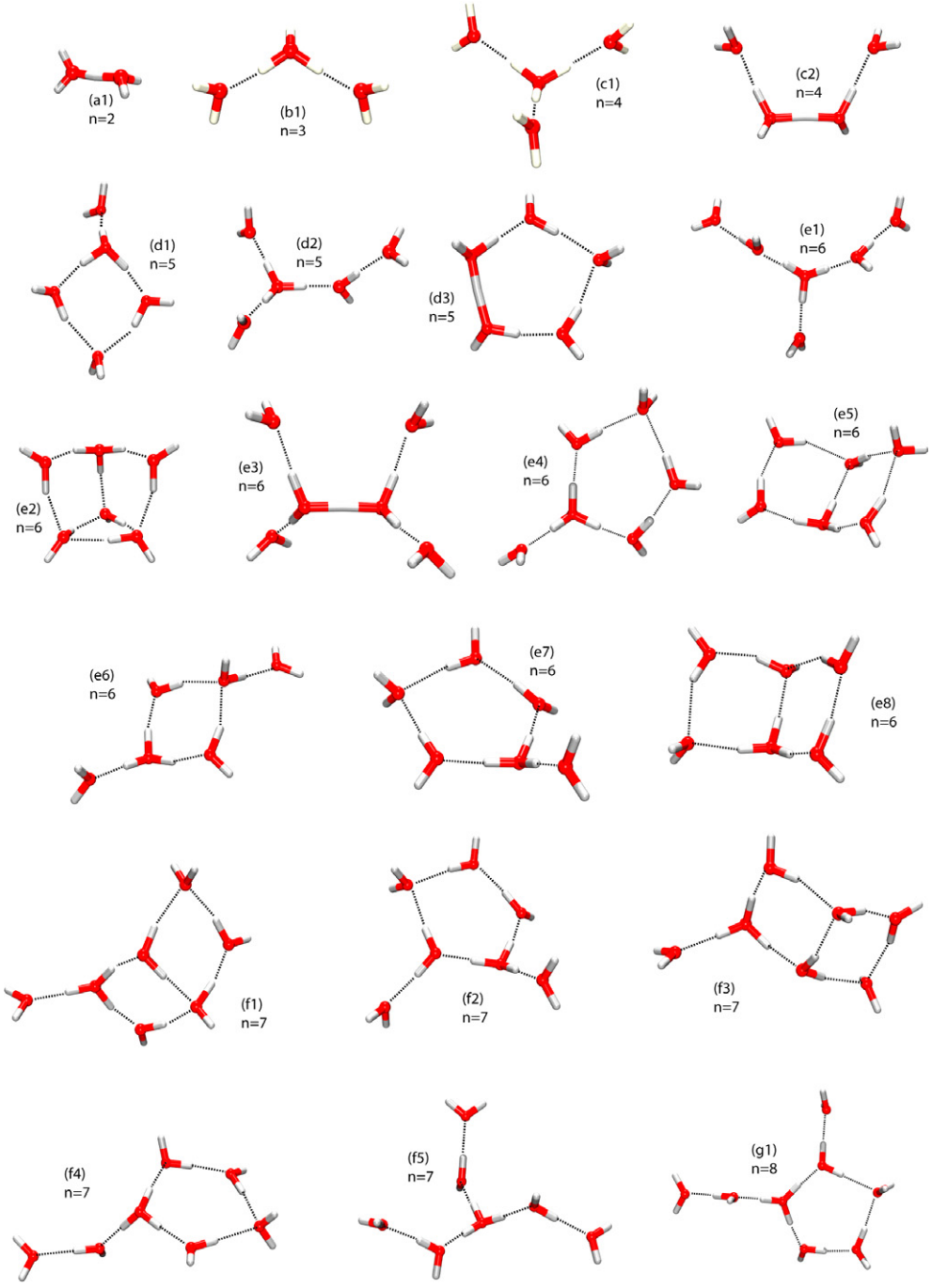

Fig. 4. MP2/6-31G(*d*) optimized geometries for protonated water clusters for $2 < n < 7$, where n is the number of waters in each cluster and the term in parenthesis refers to the individual isomers (e.g., for $n = 5$ there are 3 isomers, d1, d2, d3).

new water molecule is introduced into the cluster. As can be seen in Fig. 4, the first solvation shell closes at $n = 4$ yielding a fully hydrated Eigen-type cluster $H^+(H_2O)_4$ (Fig. 4, **c1**).

Considering the hydration step (3,4), that is

$$H^+(H_2O)_3{}^+H_2O \rightarrow H^+(H_2O)_4 \qquad (5)$$

our quantum chemical calculations reveal that hydration of the **b1** structure toward the $H^+(H_2O)_4$ isomer **c2** is around 13 kJ mol^{-1} more endergonic than the formation of isomer **c1** from **b1**. We therefore anticipate that the break in slope in Fig. 6 at $n = 4$ corresponds to extra stabilization due to closure of the first Eigen-type hydration shell and does not reflect the hydration of a Zundel-type moiety. From Table 2 and Fig. 6, it may be seen that experimental hydration enthalpies for the (3,4) step are in excellent agreement with CBS-*x*, G3 and G3B3 type *ab initio* calculations.

The addition of a fourth water molecule to H_3O^+ (step 4, 5) according to the reaction

Table 1
Calculated complete basis set (CBS-Q) enthalpies, free energies (Hartrees) and relative energies (kJ mol^{-1}) with respect to the most stable isomer (e.g., the $H_3O^+{\cdot}(H_2O)_5$ isomer **e1** lies 2.7 kJ mol^{-1} above isomer **e3**)

Cluster	Isomer	CBS-Q		
		Enthalpy	Free energy	Relative energy
H_2O		−76.332698	−76.354052	—
H_3O^+		−76.591736	−76.613728	—
$H_3O^+ \cdot (H_2O)$	**a1**	−152.977792	−153.008782	—
$H_3O^+ \cdot (H_2O)_2$	**b1**	−229.344259	−229.383975	—
$H_3O^+ \cdot (H_2O)_3$	**c1**	−305.705434	−305.754913	13.5
	c2	−305.700765	−305.749766	0.0
$H_3O^+ \cdot (H_2O)_4$	**d1**	−382.057710	−382.112024	11.1
	d2	−382.056961	−382.116267	0.0
	d3	−382.053162	−382.106383	26.0
$H_3O^+ \cdot (H_2O)_5$	**e1**	−458.407228	−458.476897	2.7
	e2	−458.406855	−458.464575	35.0
	e3	−458.407714	−458.477911	0.0
	e4	−458.408365	−458.471509	16.8
	e5	−458.405508	−458.466785	29.2
	e6	−458.407983	−458.471769	16.1
	e7	−458.407199	−458.476398	4.0
	e8	−458.404435	−458.463025	39.1
$H_3O^+ \cdot (H_2O)_6$	**f1**	−534.757957	−534.826325	23.4
	f2	−534.757218	−534.830389	12.7
	f3	−534.757963	−534.826313	23.4
	f4	−534.757730	−534.830922	11.3
	f5	−534.755730	−534.835231	0.0
$H_3O^+ \cdot (H_2O)_7$	**g1**	−611.105294	−611.188711	—

$$H^+(H_2O)_4 + H_2O \rightarrow H^+(H_2O)_5 \quad (6)$$

yields three low energy isomers **d1**, **d2**, and **d3**. The non-cyclic structure **d2** was calculated by CBS-Q, and G3 theory to be lower in energy than **d1** by 11.1 and 10.4 kJ mol^{-1}, respectively. Note that a recent IR-predissociation study by Headrick et al. (2005) for $n = 5$ observed characteristic vibrational features for a non-cyclic cluster with an Eigen-type geometry thus lending support to our claim that **d2** is the principal $H^+(H_2O)_5$ species.

Results from recent mass-selective IR spectroscopic studies (Jiang et al., 2000; Headrick et al., 2005) on the (5,6) proton hydration reaction

$$H^+(H_2O)_5 + H_2O \rightarrow H^+(H_2O)_6 \quad (7)$$

point toward two principal coexisting $H^+(H_2O)_6$ isomers: one where the Eigen core ion is hydrated by 5 water molecules and a second in which 4 water molecules reside at the terminal positions of the Zundel core ion. Christie and Jordan (2002) have studied the $H^+(H_2O)_6$ system in great detail using parallel tempering Monte Carlo simulations. The authors concluded that $H^+(H_2O)_6$ structures based on the Zundel core ion are preferred at low temperatures (<140 K) whereas Eigen-type geometries are more abundant at higher temperatures. Our CBS-Q and G3 calculations reveal two principal low lying $H^+(H_2O)_6$ isomers, the Eigen-type **e1** and Zundel-type **e3** structure following the (5,6) hydration step (Fig. 4). The **e3** ion geometry was calcuated at the CBS-Q and G3 theory level to lie 2.7 kJ mol^{-1} and 0.5 kJ mol^{-1}, respectively, below the **e1** geometry. In contrast, calculation using the G3B3 and CBS-QB3 level calculations demonstrate that the **e1** ion

Table 2
Comparison of calculated and experimental enthalpy $-\Delta H_{n,n+1}$ (kJ mol^{-1}) and entropy $-\Delta S_{n,n+1}$ (J K^{-1} mol^{-1}) values for proton (p) hydration reactions; the notation (n, $n+1$) refers to stepwise addition of water to a cluster ion (i.e., 1,2 refers to the addition of one water (w) molecule to the hydronium (h) ion)

	Experimental		Computational					
$n,n+1$	T/K	$-\Delta H$ $-\Delta S$	Geom.	CBS-Q $-\Delta H$ $-\Delta S$	CBS-QB3	CBS-APNO	G3	G3B3	B3LYP
0,1	480[a]	690.8 ± 2.9[a]	*wp → k*	686.3	686.0	691.1	689.7	689.3	710.6
		103.3 ± 4.2[a]		*103.2*	*104.1*	*94.7*	*104.2*	*104.3*	*14.3*
1,2	660–809	133.7 ± 1.7	*hw → al*	140.1	141.9	143.0	139.6	142.2	165.3
		105.0 ± 5.0		*108.8*	*114.3*	*117.1*	*95.5*	*114.8*	*108.9*
2,3	421–590	89.9 ± 1.3	*a1 → b1*	88.7	89.3	89.2	89.7	88.9	105.8
		104.7 ± 4.2		*111.2*	*101.9*	*110.6*	*106.8*	*103.6*	*92.5*
3,4	346–470	76.6 ± 1.7	*b1 → c1*	74.8	72.3	74.9	75.9	74.0	88.0
		120.7 ± 4.2		*102.1*	*117.6*	*101.1*	*107.3*	*122.4*	*112.3*
4,5	281–346	59.6 ± 1.7	*c1 → d2*	49.4	49.3	—	50.5	50.6	65.4
		122.7 ± 4.2		*101.5*	*107.9*	—	*101.3*	*107.9*	*109.4*
5,6	251–297	53.2 ± 1.7	*d2 → e1*	46.1	45.3	—	46.3	43.2	60.0
		123.1 ± 5.0		96.8	*98.2*	—	98.1	98.8	*101.0*
6,7	251–269	68.2 ± 2.5	*e3 → f5*	40.2	—	—	—	—	—
		198.3 ± 5.0		*106.1*	—	—	—	—	—
			e1 → f1	47.3	—	—	—	—	73.7
				799.5	—	—	—	—	196.1
7,8	—	—	*f1 → g1*	38.4	—	—	—	—	43.8
		—		55.6	—	—	—	—	52.4

[a] McIntosh et al. (1988).

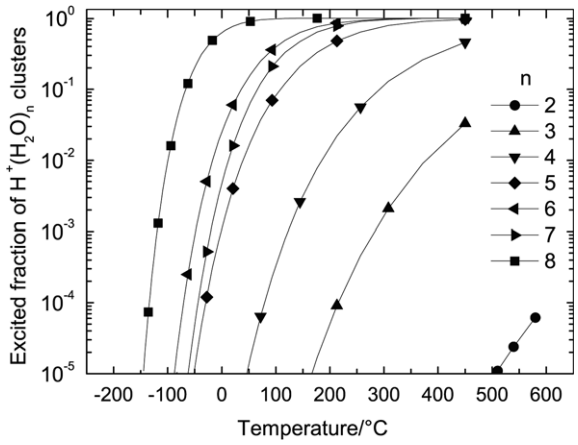

Fig. 5. Fraction of protonated water clusters with energies exceeding the dissociation threshold; n is the number of water molecules in the cluster ion.

is lower in energy than the **e3** by 1.5 kJ mol^{-1} and 4.9 kJ mol^{-1}, respectively. The CBS-Q energy difference corresponds to a Boltzmann population ratio $(N_{e1}/N_{e3}) = \exp(-\Delta E/k_B T)$ of around 2.9 in favour of the Zundel-type cluster and we therefore anticipate that both Eigen and Zundel type geometries for $n = 6$ may coexist.

Our experimental data for the addition of a water molecule to the $n = 6$ moiety

$$H^+(H_2O)_6 + H_2O \rightarrow H^+(H_2O)_7 \quad (8)$$

indicate that an anomaly (i.e., increase) in both the enthalpy and entropy occurs for the 6,7 step as shown in Fig. 6. For the 6,7 step, our enthalpy change is in excellent agreement with the value of 67.3 kJ mol^{-1} obtained from multi-photon ionization mass spectrometric results by Shi et al. (1993). The increased stability and ordering of molecules for the mesh-like structure at $n = 7$ is more obvious when the experimental entropy change is considered as it is almost twice that of the previous step: i.e., 123.1 ± 5.0 J mol^{-1} K^{-1} for the (5,6) step and 198.3 ± 5.0 J mol^{-1} K^{-1} for the (6,7) step in this study. Shi et al. (1993) report both a shift toward greater exothermicity (67.3 kJ mol^{-1}) as well as an anomalously high entropic value (346.0 J mol^{-1} K^{-1}) for the (6,7) hydration step. Consequently, enthalpic and entropic changes reported by Shi et al. (1993) for the (6,7) step have been categorized in the NIST database as questionable and thus removed from the list of recommended (6,7) clustering equilibria. In addition, we note that other mass spectrometric results pertaining to protonated water clusters by Searcy and Fenn (1974), Hermann et al. (1982), Yang and Castleman (1989) and Yang et al. (1991) also indicate the presence of an anomaly at the 6,7 step. The laser ionisation study on neutral water clusters by Dong et al. (2006) provide further support for the energetic trends reported in this study (Table 2; Fig. 6). Note that Dong and coworkers have been able to reproduce measured decay fractions and binding energies of proton water clusters up to the magic number $H^+(H_2O)_{21}$.

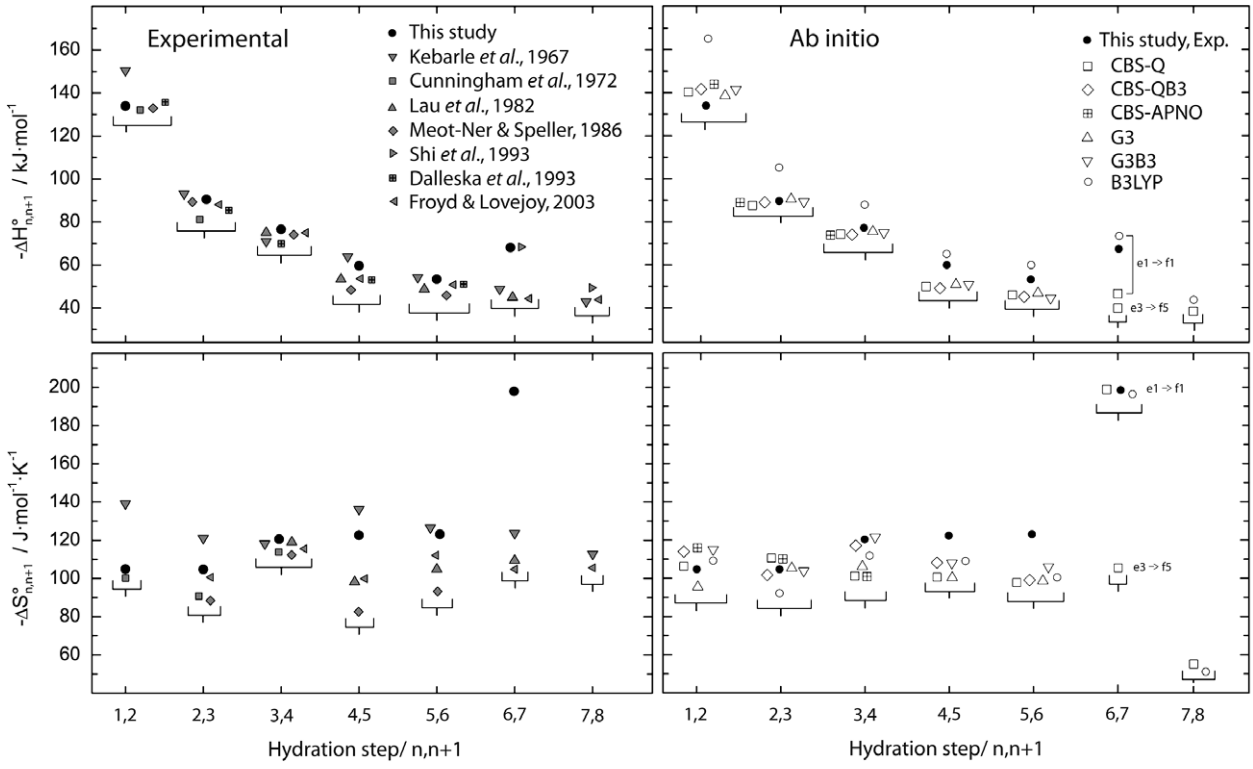

Fig. 6. Comparison of experimental and quantum chemical enthalpy and entropy changes for proton hydration reactions obtained in this study with previous experimental data. See above-mentioned references for further information.

In order to gain insight into the nature of 6,7 transition, we have carried out an extensive set of CBS-Q calculations for a number of possible reactions arising from the addition of one water molecule to the $H^+(H_2O)_6$ cluster (see Table 3). The geometries of various isomers and corresponding enthalpies and energies of formation as well as relative energies are given in Fig. 4 and listed in Table 1. The energetically most favourable hydration of $H^+(H_2O)_6$ would be from the **e3** (or **e1** and **e7**) to the **f5** cluster which results in values of -41.5 kJ mol^{-1} and -101.5 J mol^{-1} K^{-1} for the enthalpy and entropy of reaction, respectively (Table 3). These values are in agreement with the expected trends for the 6,7 step calculated for the preceding steps (Table 2) as well as for some of the earlier experimental data of Kebarle et al. (1967), Lau et al. (1982) and Froyd and Lovejoy (2003) as shown in Fig. 6. However, the *ab initio* calculated enthalpy and entropy for the 6,7 step, assuming the energetically favourable **e3** → **e5** pathway, are in poor agreement with our experimentally derived enthalpy and entropy values. The enthalpies and entropies obtained for the less favourable pathways **e1** → **f1**, **e1** → **f3**, **e3** → **f3** and **e7** → **f3** are in reasonable agreement with our experimentally derived values of $\Delta H = -68.2$ kJ mol^{-1} and $\Delta S = -198.3$ J mol^{-1} K^{-1}. The dilemma here is that we are still uncertain that the currently identified isomers for the $H^+(H_2O)_6$ and $H^+(H_2O)_7$ clusters represent the only possible configurations. We note, for example, that more than 20$H^+(H_2O)_7$ isomers have been reported (Jiang et al., 2000; Wang et al., 2003; Yamaguchi et al., 2003), however, the **f1** and **f3** isomer were not listed in these studies.

No new hydrogen bonds are formed in the (7,8) step. However, the rearrangement of the mesh-like structure at $n = 7$ into a ring formed by 5 water molecules at $n = 8$ (Ciobanu et al., 2000) adds some stabilization so that the decrease in enthalpy is not as sharp as might be expected. The stepwise enthalpy trends clearly demonstrate the competition between the weakening effect of adding a water molecule on the new and existing hydrogen bonds and the stabilizing effect of the formation of new hydrogen bonds. The magnitudes of stepwise enthalpies approach the value -45 kJ mol^{-1} for larger clusters, which is compares well with the -44.0 kJ mol^{-1} value of the molar enthalpy of condensation of water (Chase, 1998) at room temperature.

5. CONCLUSIONS

The stepwise hydration of the proton has been studied both experimentally using our high-pressure mass spectrometer and theoretically using high accuracy model chemistries as well as density-functional theory. Protonated water clusters with the number water molecules ranging from 1 to 7 have been experimentally observed and compared with high accuracy quantum chemical methods up to cluster structures with $n = 8$. Two principal aspects emerge from our study: firstly, from our experimental hydration enthalpies for small-sized ($n \leqslant 4$) protonated water clusters, we have been able to identify changes in ΔH as a function of the hydration number that stem from shell filling effects around an Eigen-type cation. CBS-Q, CBS-QB3, CBS/QCI-APNO, G3B3 and G3 level theory calculations are capable of reproducing the experimental differential enthalpies and entropies of hydration for small-sized clusters within reported errors. Secondly, we have observed experimentally a distinct discontinuity in the enthalpy and entropy of the 6,7 hydration step, although the entropy jump attending hydration reported by Shi et al. (1993) is more pronounced. Interestingly, an entropic effect has also been noted for the formation of magic number clusters $H^+(H_2O)_{21}$ (Shi et al., 1993).

Comparison of our experimental results with previous experimental data reveal discrepancies believed to stem from the improved design and accuracy of our HPMS apparatus and, on some occasions, from inappropriate experimental conditions in earlier HPMS investigations. The stepwise trends in enthalpy of proton hydration are interpreted in terms of the number of additional hydrogen bonds formed at each hydration step and the weakening

Table 3
Comparison of binding enthalpies $-\Delta H_{6,7}$ (kJ mol^{-1}) and entropies $-\Delta S_{6,7}$ (J K^{-1} mol^{-1}) for the reaction $H^+(H_2O)_6 + H_2O = H^+(H_2O)_7$ for different isomer combinations calculated at CBS-Q level of theory (e.g., values for $\Delta H_{6,7}$ and $\Delta S_{6,7}$ for the hydration of isomer **e1** to **f1** are -47.3 kJ mol^{-1} and -199.5 J K^{-1} mol^{-1}, respectively)

	$-\Delta H_{6,7}$ $-\Delta S_{6,7}$							
	e1	**e2**	**e3**	**e4**	**e5**	**e6**	**e7**	**e8**
f1	47.3	48.3	46.1	44.4	51.9	45.4	47.4	54.6
	199.5	*94.3*	*204.2*	*142.0*	*125.6*	*147.7*	*101.9*	*101.9*
f2	45.4	46.4	44.1	42.4	49.9	43.4	45.5	52.7
	157.2	*52.0*	*161.9*	*99.7*	*83.3*	*105.4*	*157.2*	*59.6*
f3	47.4	48.3	46.1	44.4	51.9	45.4	47.3	54.7
	199.6	*94.4*	*204.3*	*142.2*	*125.8*	*147.9*	*195.5*	*102.1*
f4	46.7	47.7	45.5	43.8	51.3	44.8	46.8	54.1
	157.0	*51.8*	*161.7*	*99.6*	*83.1*	*105.2*	*152.9*	*59.5*
f5	41.5	42.5	40.2	38.5	46.0	39.5	41.6	48.8
	101.5	*3.8*	*106.1*	*44.0*	*27.6*	*49.7*	*97.3*	*3.9*

effect of an increasing cluster size on ion–solvent interactions. However, the macroscopic thermochemical parameters merely reflect a complex shifting balance amongst vibrational, translational and rotational contributions to the overall cluster stability (Gilligan and Castleman, 2003). We also note that our experimental total hydration energy following attachment of six water molecules to the H_3O^+ ion is exergonic by around 250.1 kJ mol^{-1} which constitutes around 65% of the total bulk hydration energy of H_3O^+ in liquid water (i.e., −383.1 kJ mol^{-1}) (McIntosh et al., 1988; Pliego and Riveros, 2002).

ACKNOWLEDGMENTS

TMS is grateful to the Swiss National Science Foundation and the ETH Research Commission for grants supporting this research.

REFERENCES

Aplin K. L., and McPheat R. A. (2005) Absorption of infra-red radiation by atmospheric molecular cluster-ions. *J. Atmos. Sol.-Terr. Phys.* **67**, 775–783.

Archibald S. M., Migdisov A. A., and Williams-Jones A. E. (2002) An experimental study of the stability of copper chloride complexes in water vapor at elevated temperatures and pressures. *Geochim. Cosmochim. Acta* **66**, 1611–1619.

Armellini F. J., and Tester J. W. (1993) Solubility of sodium chloride and sulfate in sub- and supercritical water vapor from 450 to 550 °C and 100 to 250 bar. *Fluid Phase Equilibr.* **84**, 123–142.

Asmis K. R., Pivonka N. L., Santambrogio G., Brummer M., Kaposte C., Neumark D. M., and Woste L. (2003) Gas-phase infrared spectrum of the protonated water dimer. *Science* **299**, 1375–1377.

Baboul A. G., Curtiss L. A., Redfern P. C., and Raghavachari K. (1999) Gaussian-3 theory using density functional geometries and zero-point energies. *J. Chem. Phys.* **110**, 7650–7657.

Bischoff J. L., and Rosenbauer R. J. (1986) The system NaCl-H_2O: Relations of vapor–liquid near the critical temperature of water and of vapor–liquid-halite from 300 °C to 500 °C. *Geochim. Cosmochim. Acta* **50**, 1437–1444.

Carlon H. R. (1979) Do clusters contribute to the infrared-absorption spectrum of water vapor? *Infrared Phys.* **19**, 547–549.

Carlon H. R. (1980) Ion content of air humidified by boiling water. *J. Appl. Phys.* **51**, 171–173.

Carlon H. R. (1982) New measurements of the ion content of evaporation-humidified air. *J. Chem. Phys.* **76**, 5523–5529.

Chang H. C., Wu C. C., and Kuo J. L. (2005) Recent advances in understanding the structures of medium-sized protonated water clusters. *Int. Rev. Phys. Chem.* **24**, 553–578.

Chase M. W. (1998) NIST-JANAF themochemical tables. *J. Phys. Chem. Ref. Data* **9**, 1–1951.

Christie R. A., and Jordan K. D. (2001) Theoretical investigation of the $H_3O^+(H_2O)_4$ cluster. *J. Phys. Chem. A* **105**, 7551–7558.

Christie R. A., and Jordan K. D. (2002) Finite temperature behaviour of $H^+(H_2O)_6$ and $H^+(H_2O)_8$. *J. Phys. Chem. B* **106**, 8376–8381.

Ciobanu C. V., Ojamäe L., Shavitt I., and Singer S. J. (2000) Structure and vibrational spectra of $H^+(H_2O)_8$: Is the excess proton in a symmetrical hydrogen bond? *J. Chem. Phys.* **113**, 5321–5330.

Cunningham A. J., Payzant J. D., and Kebarle P. (1972) Kinetic study of proton hydrate $H^+(H_2O)_n$ equilibria in gas-phase. *J. Am. Chem. Soc.* **94**, 7627–7632.

Curtiss L. A., Frurip D. J., and Blander M. (1979) Studies of molecular association in H_2O and D_2O vapors by measurement of thermal conductivity. *J. Chem. Phys.* **71**, 2703–2727.

Curtiss L. A., Raghavachari K., Trucks G. W., and Pople J. A. (1991) Gaussian-2 theory for molecular energies of 1st-row and 2nd-row compounds. *J. Chem. Phys.* **94**, 7221–7230.

Curtiss L. A., Raghavachari K., Redfern P. C., Rassolov V., and Pople J. A. (1998) Gaussian-3 theory for molecular energies of first- and second-row compound. *J. Chem. Phys.* **109**, 7764–7776.

Dalleska N. F., Honma K., and Armentrout P. B. (1993) Stepwise solvation enthalpies of protonated water clusters: collision-induced dissociation as an alternative to equilibrium studies. *J. Am. Chem. Soc.* **115**, 12125–12131.

Diri K., Myshakin E. M., and Jordan K. D. (2005) On the contribution of vibrational anharmonicity to the binding energies of water clusters. *J. Phys. Chem. A* **109**, 4005–4009.

Dong F., Heinbuch S., Rocca J. J., and Bernstein E. R. (2006) Dynamics and fragmentatiom of van der Waals clusters: $(H_2O)_n$, $(CH_3OH)_n$, and $(NH_3)_n$ upon ionization by a 26.5 eV Soft X-ray laser. *J. Chem. Phys.* **124**, 224319.

Dunning T. H. (2000) A road map for the calculation of molecular binding energies. *J. Phys. Chem. A* **104**, 9062–9080.

Eigen M. (1963) Protonenübertragung, Säure-Base-Katalyse und enzymatische Hydrolyse . 1. Elementarvorgänge. *Angew. Chem.* **75**, 489–508.

Eigen M., and De Maeyer L. (1958) Self-dissociation and protonic charge transport in water and ice. *Proc. Roy. Soc. (Lond.) A* **247**, 505–533.

Ferguson E. E., and Arnold F. (1981) Ion chemistry of the stratosphere. *Acc. Chem. Res.* **14**, 327–334.

Ferguson E. E., and Fehsenfeld F. C. (1969) Water vapor ion cluster concentration in the D region. *J. Geophys. Res.* **74**, 5743–5751.

Frisch, M.J., Trucks, G.W., Schlegel, H.B., Scuseria, G.E., Robb, M.A., Cheeseman, J.R., Zakrzewski, V.G., Montgomery, J.A., Stratmann, R.E., Burant, J.C., Dapprich, S., Millam, J.M., Daniels, A.D., Kudin, K.N., Strain, M.C., Farkas, O., Tomasi, J., Barone, V., Cossi, M., Cammi, R., Mennucci, B., Pomelli, C., Adamo, C., Clifford, S., Ochterski, J., Petersson, G.A., Ayala, P.Y., Cui, Q., Morokuma, K., Malick, D.K., Rabuck, A.D., Raghavachari, K., Foresman, J.B., Cioslowski, J., Ortiz, J.V., Stefanov, B.B., Liu, G., Liashenko, A., Piskorz, P., Komaromi, I., Gomperts, R., Martin, R.L., Fox, D.J., Keith, T., Al-Laham, M.A., Peng, C.Y., Nanayakkara, A., Gonzalez, C., Challacombe, M., Gill, P.M.W., Johnson, B., and Chen, W. (2003) GAUSSIAN03, Revision C.02, Gaussian Inc., Pittsburgh, PA.

Froyd K. D., and Lovejoy E. R. (2003) Experimental thermodynamics of cluster ions composed of H_2SO_4 and H_2O.1. Positive ions. *J. Phys. Chem. A* **46**, 9800–9811.

Gilligan J. J., and Castleman A. W. (2003) Solvation effects on the properties and reactivities of ionic and neutral water clusters. In *Water in Confining Geometries* (eds. V. Buch and J. P. Devlin). Springer Series in Cluster Physics, pp. 101–138.

Headrick J. M., Diken E. G., Walters R. S., Hammer N. I., Christie R. A., Cui J., Myshakin E. M., Duncan M. A., Johnson M. A., and Jordan K. D. (2005) Spectral signatures of hydrated proton vibrations in water clusters. *Science* **308**, 1765–1769.

Heinrich C. A., Günther D., Audetat A., Ulrich T., and Frischknecht R. M. (1999) Metal fractionation between magmatic brine and vapor, determined by microanalysis of fluid inclusions. *Geology* **27**, 755–758.

Hermann V., Kay B. D., and Castleman A. W. (1982) Evidence for the existence of structures in gas-phase homomolecular clusters of water. *Chem. Phys.* **72**, 185–200.

Hiraoka K., Takimoto H., and Morise K. (1986) Gas-phase hydration reactions of Protonated alcohols. Energetics and bulk hydration of cluster ions. *J. Am. Chem. Soc.* **108**, 5683–5689.

Hiraoka K., Mizuse S., and Yamabe S. (1988) Solvation of halide ions with H_2O and CH_3CN in the gas-phase. *J. Am. Chem. Soc.* **92**, 3943–3952.

Jiang J. C., Chang H.-C., Wang Y.-S., Lin S. H., Lee Y. T., Niedner-Schatteburg G., and Chang H.-C. (2000) Infrared spectra of $H^+(H_2O)_{5-8}$ clusters: Evidence for symmetric proton hydration. *J. Am. Chem. Soc.* **122**, 1398–1410.

Kalinichev A. G., and Churakov S. V. (2001) Thermodynamics and structure of molecular clusters in supercritical water. *Fluid Phase Equilibr.* **183**, 271–278.

Kebarle P., Searles S. K., Zolla A., Scarborough J., and Arshadi M. (1967) Solvation of hydrogen ion by water molecules in gas phase. Heats and entropies of solvation of individual reactions $H^+(H_2O)_{n-1} + H_2O = H^+(H_2O)_n$. *J. Am. Chem. Soc.* **89**, 6393–6399.

Klemperer W., and Vaida V. (2006) Molecular complexes in close and far away. *Proc. Natl. Acad. Sci.* **103**, 10584–10588.

Klots C. E. (1984) The pH of steam. *J. Phys. Chem.* **88**, 4407–4410.

Kochanski E., Kelterbaum R., Klein S., Rohmer M. M., and Rahmouni A. (1997) Decades of theoretical work on protonated hydrates. *Adv. Quantum Chem.* **28**, 273–291.

Kuo J. L., and Klein M. L. (2005) Structure of protonated water clusters: low-energy structures and finite temperature behavior. *J. Chem. Phys.* **122**, 024516.

Lau Y. K., Ikuta S., and Kebarle P. (1982) Thermodynamics and kinetics of the gas-phase reactions—$H_3O^+(H_2O)_{n-1} + H_2O = H_3O^+(H_2O)_n$. *J. Am. Chem. Soc.* **104**, 1462–1469.

Lemke K. H., and Seward T. M. (2006) Ab initio calculations of solvation processes in volcanic gases. *Eos Trans. AGU Fall Meet. Suppl.*, V53A–V1733 (abstr.).

Lide D. R. (1996) *CRC Handbook of Chemistry and Physics*. CRC Press.

Likholyot A., Hovey J. K., and Seward T. M. (2005a) New high pressure mass spectrometer with improved reaction temperature measurement. *Int. J. Mass Spectrom.* **243**, 49–62.

Likholyot A., Hovey J. K., and Seward T. M. (2005b) Experimental and theoretical study of hydration of halide ions. *Geochim. Cosmochim. Acta* **69**, 2949–2958.

Lin C. K., Wu C. C., Wang Y.-S., Lee Y. T., Chang H.-C., Kuo J. L., and Klein M. L. (2005) Vibrational predissociation spectra and hydrogen-bond topologies of $H^+(H_2O)_{(9-11)}$. *Phys. Chem. Chem. Phys.* **7**, 938–944.

Mao W. L., and Mao H-k. (2004) Hydrogen storage in molecular compounds. *Proc. Natl. Acad. Sci.* **101**, 708–710.

Marx D. (2006) Proton transfer 200 years after von Grotthuss: Insights from ab initio simulations. *Chem. Phys. Chem.* **7**, 1848–1870.

Marx D., Tuckerman M. E., Hutter J., and Parrinello M. (1999) The nature of the hydrated excess proton in water. *Nature* **397**, 601–604.

Masamura M. (2001) The effect of basis set superposition error on the convergence of interaction energies. *Theor. Chem. Acc.* **106**, 301–313.

Matubayasi N., Wakai C., and Nakahara M. (1997) Structural study of supercritical water. I. Nuclear magnetic resonance spectroscopy. *J. Chem. Phys.* **107**, 9133–9140.

Mayer P. M. (1999) Benchmark enthalpies of formation and binding energies of proton-bound pairs between HCN and HCN, NH_3, H_2O, and HF. *J. Chem. Phys.* **110**, 7779–7788.

McIntosh B. J., Adams N. G., and Smith D. (1988) Determination of the proton affinities of H_2O and CS_2 relative to C_2H_4. *Chem. Phys. Lett.* **148**, 142–148.

Mella M., Kuo J. L., Clary D. C., and Klein M. L. (2005) Nuclear quantum effects on the structure and energetics of $(H_2O)_{(6)}H^+$. *PCCP* **7**, 2324–2332.

Meot-Ner M. (2005) The ionic hydrogen bond. *Chem. Rev.* **105**, 213–284.

Meot-Ner M., and Field F. H. (1977) Stability, association and dissociation in the cluster ions $H_3S^+ \cdot nH_2S$, $H_3O^+ \cdot nH_2O$ and $H_2S^+ \cdot H_2O$. *J. Am. Chem. Soc.* **99**, 998–1003.

Meot-Ner M., and Speller C. V. (1986) The filling of solvent shells in cluster ions: Thermochemical criteria and the effects of isomeric clusters, J. *Phys. Chem.* **90**, 6616–6624.

Meot-Ner M., Scheiner S., and Yu W. O. (1998) Ionic hydrogen bonds in bioenergetics. 3. Proton transport in membranes, modeled by ketone/water clusters. *J. Am. Chem. Soc.* **120**, 6980–6990.

Miyazaki M., Fujii A., Ebata T., and Mikami N. (2004) Infrared spectroscopic evidence for protonated water clusters forming nanoscale cages. *Science* **304**, 1134–1137.

Montgomery J. A., Ochterski J. W., and Petersson G. A. (1994) A complete basis set model chemistry. IV. An improved atomic pair natural orbital method. *J. Chem. Phys.* **101**, 5900–5909.

Montgomery J. A., Frisch M. J., Ochterski J. W., and Petersson G. A. (1999) A complete basis set model chemistry. VI. Use of density functional geometries and frequencies. *J. Chem. Phys.* **110**, 2822–2827.

Nyden M. R., and Petersson G. A. (1981) Complete basis set correlation energies. I. The asymptotic convergence of pair natural orbital expansions. *J. Chem. Phys.* **75**, 1843–1862.

Ochterski J. W., Petersson G. A., and Montgomery J. A. (1996) A complete basis set model chemistry. V. Extensions to six or more heavy atoms. *J. Chem. Phys.* **104**, 2598–2619.

Pfeilsticker K., Lotter A., Peters C., and Bösch H. (2003) Atmospheric detection of water dimers via near-infrared absorption. *Science* **300**, 2078–2080.

Pickard F. C., Pokon E. K., Liptak M. D., and Shields G. C. (2005) Comparison of CBS-QB3, CBS-APNO, G2, and G3 thermochemical predictions with experiment for formation of ionic clusters of hydronium and hydroxide ions complexed with water. *J. Chem. Phys.* **122**, 24302.

Pliego J. R., and Riveros J. M. (2002) Gibbs energy of solvation of organic ions in aqueous and dimethyl sulfoxide solutions. *Phys. Chem. Chem. Phys.* **4**, 1622–1627.

Pulinets S., and Boyarchuk K. (2004) *Ionospheric Precursors of Earthquakes*. Springer Books, Berlin, pp. 315.

Pulinets S. A., Ouzounov D., Ciraolo L., Singh R., Cervone G., Leyva A., Dunajecka M., Karelin A. V., Boyarchuk K. A., and Kotsarenko A. (2006) Thermal, atmospheric and ionospheric anomalies around the time of the Colima M7.8 earthquake of 21 January 2003. *Ann. Geophys.* **24**, 835–849.

Schaftenaar G., and Noordik J. H. (2000) Molden: a pre- and post-processing program for molecular and electronic structures. *J. Comput.-Aided Mol. Des.* **14**, 123–134.

Searcy J. Q., and Fenn J. B. (1974) Clustering of water on hydrated protons in a supersonic free jet expansion. *J. Chem. Phys.* **61**, 5282–5288.

Sennikov P., Ignatov S. K., and Schrems O. (2005) Complexes and clusters of water relevant to atmospheric chemistry: H_2O complexes with oxidants. *Chem. Phys. Chem.* **6**, 392–412.

Shi Z., Ford V., Wei S., and Castleman A. W. (1993) Water clusters—contributions of binding energy and entropy to stability. *J. Chem. Phys.* **99**, 8009–8015.

Shin J. W., Hammer N. I., Diken E. G., Johnson M. A., Walters R. S., Jaeger T. D., Duncan M. A., and Christie R. A. (2004) Infrared signature of structures associated with the $H^+(H_2O)_{(n)}$ ($n = 6$ to 27) clusters. *Science* **304**, 1137–1140.

Stein S. E., and Rabinovitch B. S. (1973) Accurate evaluation of internal energy level sums and densities including anharmonic oscillators and hindered rotors. *J. Chem. Phys.* **58**, 2438–2445.

Suleimenov, O.M. and Seward, T.M. (2006) Sodium chloride–water clusters in steam: classical, quantum chemical and thermodynamic computational approach. Goldschmidt Meeting, 2006, Melbourne, Australia, (abstr.).

Sunner J., and Kebarle P. (1981) Unimolecular dissociation of ions—effect on mass spectrometric measurements of ion-molecule association equilibria. *J. Phys. Chem.* **85**, 327–335.

Vaida V., Tuck A. F., Goss L. M., Daniel J. S., and Kjaergaard H. (2001) The role of water dimers in atmospheric radiative transfer: near IR/visible vibrational overtone spectra. *Q. J. Roy. Met. Soc.* **127**, 1627–1643.

Wang Y. S., Tsai C. H., Lee Y. T., Chang H. C., Jiang J. C., Asvany O., Schlemmer S., and Gerlich D. (2003) Investigations of protonated and deprotonated water clusters using a low-temperature 22-pole ion trap. *J. Phys. Chem. A* **107**, 4217–4225.

Williams-Jones A. E., Migdisov A. A., Archibald S. M., and Xiao Z. (2002). In Vapor transport of ore metals ion (eds. R. Hellmann and S. A. Wood). *Geochem. Soc. Spec. Publ.* **7**, 279–305.

Wu C. C., Lin C. K., Chang H. C., Jiang J. C., Kuo J. L., and Klein M. L. (2005) Protonated clathrate cages enclosing neutral water molecules: $H^+(H_2O)_{(21)}$ and $H^+(H_2O)_{(28)}$. *J. Chem. Phys.* **122**, 07431.

Xantheas, S. S. (2005) Interactions potentials for water from accurate cluster calculations. In *Intermolecular Forces and Clusters II. Structure and Bonding* (ed. D. J. Wales) Springer, p. 116.

Yamaguchi S., Kudoh S., Okada Y., Orii T., Takeuchi K., Ichikawa T., and Nakai H. (2003) Size-dependent reaction cross section of protonated water clusters $H^+(H_2O)_{(n)}$ ($n = 2$–11) with D_2O. *J. Phys. Chem. A* **107**, 10904–10910.

Yang X., and Castleman A. W. (1989) Large protonated water clusters $H^+(H_2O)_n$, ($1 = n > 60$): the production and reactivity of clathrate-like structures under thermal conditions. *J. Am. Chem. Soc.* **111**, 6845–6846.

Yang X., Zhang X., and Castleman A. W. (1991) Kinetics and mechanism studies of large protonated water clusters, $H^+(H_20)_n$, $n = 1$–60, at thermal energy. *Int. J. Mass Spect. Ion Proc.* **109**, 339–354.

Zundel G., and Metzer H. (1968) Energy bands of excess tunneling protons in fluid acids. IR spectroscopy of $H_5O_2^+$ groups. *Z. Phys. Chem.* **58**, 225.

Associate editor: William H. Casey